

Neural Network based Post-Equalization in Optical Coherent Systems: Regression versus Classification

Pedro J. Freire, Jaroslaw E. Prilepsky, Yevhenii Osadchuk, Sergei K. Turitsyn, Vahid Aref

Abstract—In this paper, we address the question of which type of predictive modeling, classification, or regression, fits better the task of equalization using neural networks (NN) based post-processing in coherent optical communication, where the transmission channel is nonlinear and dispersive. For the first time, we presented some possible drawbacks in using each type of predictive task in a machine learning context for the nonlinear channel equalization problem. We studied two types of equalizers based on the feed-forward and recurrent neural networks over several different transmission scenarios, in linear and nonlinear regimes of the optical channel. We observed in all those cases that the training based on regression results in faster convergence and finally a superior performance, in terms of Q-factor and achievable information rate.

Index Terms—Neural networks, nonlinear equalizer, classification, regression, coherent detection, digital signal processing, optical communications.

I. INTRODUCTION

TO improve the performance of optical fiber systems it is important to mitigate the detrimental impact of linear and, most importantly, nonlinear transmission impairments that cap the systems' throughput [1]–[3]. Numerous digital signal processing (DSP) algorithms have been proposed and studied [3] for optical fiber channel equalization. The most popular approach is the receiver-based equalizer – a special-purpose DSP device that can (partially) reverse the distortions incurred by a signal when passing over the optical channel. These equalizers are typically designed and optimized based on the minimum-mean-squared-error (MMSE) criteria. The usefulness of MMSE equalizers is stipulated by several reasons, including (i) the mean squared error minimization is an optimal condition for the transmission over the additive white Gaussian noise (AWGN) channel; (ii) the MMSE is quite convenient for mathematical optimization because of convexity and differentiability of its objective function; and (iii) the MMSE equalizer is usually optimized independently of the underlying waveform or modulation format.

Another approach is to design an equalizer as a classifier, as in digital communications the transmitted signal is usually

generated from a discrete finite-size constellation, e.g. quadrature amplitude modulation, QAM. This approach has received more attention recently, e.g. [4]–[7], because of the following main reasons: (i) the classifier is optimized for the specific in-use modulation format; (ii) it directly maximizes the information rate, the main objective of the channel equalization, and outputs the likelihoods for each received symbol, a more suitable metric for the subsequent forward error correction; (iii) and, even more importantly, it can adapt itself to the correct statistical channel characteristics.

Over the past few years, the “conventional equalizers” have started to evolve toward the designs incorporating machine learning techniques [8]–[10]. In particular, the neural network (NN) based channel equalization has recently become a topic of intensive research in optical communications, due to its capability in mitigation of linear and nonlinear impairments in optical channel and transceivers [7], [11]–[20]. Additionally, the end-to-end learning designs [4] that deal with coherent constellation optimization have been intensively studied in the literature [21]–[26] by using the traditionally auto-encoder configuration which is usually trained as a classifier. We should emphasize at this point that the transfer of the methods developed in the field of machine learning to optical communications should take into account *the underlying peculiarities and challenges of NN algorithms themselves*, while those are often overlooked when designing the equalizers. In particular, there has been no prescription whether to design NN equalization based on regression or classification with analytical or numerical comparison in terms of training complexity or eventual performance.

A fair comparison between regression and classification is quite challenging, as they produce different output variable types: discrete versus continuous, respectively. Such comparison studies exist to some extent in the machine learning area where the logistic regression accuracy is compared to that rendered by the classification [27], [28], or the output of the classification with the different loss functions is analyzed [29]–[31]. However, to our knowledge, only in [32] the motivation of solving problems with regression instead of classification was directly explained for some specific problems. In [33]–[38] it was recognized that both regression and classification tasks have potential downsides: the regression model cannot utilize the flexibility of discriminative NN models; the classification model, in turn, is not able to capture the value of difference when we misinterpret the classes, which can degrade the modeling quality. Thus, in these works, the combination of the regression and classification was proposed as the best problem fit. This approach was coined the joint

This paper was supported by the EU Horizon 2020 program under the Marie Skłodowska-Curie grant agreement 813144 (REAL-NET). JEP is supported by Leverhulme Trust, Grant No. RP-2018-063. SKT acknowledges support of the EPSRC project TRANSNET

Pedro J. Freire, Yevhenii Osadchuk, Jaroslaw E. Prilepsky and Sergei K. Turitsyn are with Aston Institute of Photonic Technologies, Aston University, United Kingdom, p.freiredecarvalhosouza@aston.ac.uk.

Vahid Aref is with Nokia, Lorenzstraße 10, 70435, Stuttgart, Germany, vahid.aref@nokia.com.

Manuscript received xxx 19, zzz; revised January 11, yyy.

classification-regression learning.

The interest in finding the optimum solution between the regression- and classification-based equalization-type algorithms, frequently arising in different areas, prompts us to conduct the investigation of this dilemma for the development of NN-based equalizers in coherent optical systems. For the optical channel equalization, this comparison may be made more evident by contrasting the classification output to that obtained with the regression in terms of bit error rate (BER) (i.e. using a hard decision metric) and the achieved mutual information (MI) (i.e. using a soft decision metric). In this paper, we compare the performance of classification and regression predictive models and expose the potential drawbacks of each task for the NN-based optical channel equalization that can explain our findings quantitatively.

II. NEURAL NETWORK-BASED EQUALIZERS

A. Regression-based and Classification-based Equalizers

Equalization is the task of recovering the transmitted data X_n from the received data Y_n . It maps Y_n to the most likely transmitted data $\hat{X}_n = f(Y_n; \Theta)$ for a given mapping function $f(\cdot)$ and the set of trainable parameters Θ , optimized according to some likelihood measure. In our case of NN-based equalization, $f(\cdot; \Theta)$ denotes the neural network itself and Θ denotes its trainable weights and parameters. Here, X_n and Y_n can denote either a single sample of transmitted and received data or sequences of samples. For simplicity of presentation, we assume the former and assume that X_n is chosen from a constellation $\{c_1, c_2, \dots, c_m\}$ with $c_i \in \mathbb{C}$, the complex space.

In regression-based equalization, $f(Y_n; \Theta)$ is relaxed to output any complex value and its likelihood maximization boils down to the minimization of mean square error, i.e.

$$\Theta_{\text{reg}}^* = \operatorname{argmin}_{\Theta} \left\{ \mathbb{E}_{X_n, Y_n} [|X_n - f(Y_n; \Theta)|^2] \right\}. \quad (1)$$

The above expectation is over samples of transmitted data and the corresponding received data. Those samples are in fact distributed according to $P(X_n, Y_n) = P(X_n)P(Y_n|X_n)$, where $P(X_n)$ is the transmitted signal distribution and $P(Y_n|X_n)$ describes how likely the channel outputs Y_n upon transmission of X_n . Note that Θ_{reg}^* is usually found weakly sensitive to the choice of modulation format due to the relaxation of $f(Y_n; \Theta)$.

In classification-based equalization, $\hat{X}_n \in \{c_1, c_2, \dots, c_m\}$. In this case, $f(Y_n; \Theta)$ is relaxed to output a vector of posterior probabilities (q_1, \dots, q_m) where $q_k := Q(X_n = c_k|Y_n; \Theta)$ showing how likely $X_n = c_k$ given receiving Y_n . Then \hat{X}_n is c_k with the largest posterior probability. It turns out that the “maximum likelihood” estimation (the best effort of model $f(\cdot)$) is obtained if the following categorical cross entropy loss (CEL) of the actual posterior $P(X_n|Y_n)$ and $Q(X_n|Y_n; \Theta)$ is minimized, i.e.

$$\mathcal{X}(P, Q; \Theta) = -\mathbb{E}_{Y_n} \left[\sum_{k=1}^m P(c_k|Y_n) \log_2(Q(c_k|Y_n; \Theta)) \right] \quad (2)$$

Equivalently, one can instead maximize

$$I_{\Theta}(X_n; \hat{X}_n) = \mathbb{E}_X [\log_2(P(X_n))] - \mathcal{X}(P, Q; \Theta), \quad (3)$$

where $I_{\Theta}(X_n; \hat{X}_n)$ is the achievable mutual information for the mismatched decoding rule $Q(X_n|Y_n; \Theta)$ [39, Def. 12]. As a result, a classification-based equalization is optimized for,

$$\Theta_{\text{cl}}^* = \operatorname{argmax}_{\Theta} \left\{ I_{\Theta}(X_n; \hat{X}_n) \right\}. \quad (4)$$

Note that $I_{\Theta}(X_n; \hat{X}_n) \leq I(X; Y)$ the true mutual information of the channel and the equality holds if $Q(X_n|Y_n; \Theta_{\text{cl}}^*) = P(X_n|Y_n)$ for all (X_n, Y_n) .

In the case of regression-based equalization, the mutual information (MI) cannot be expressed directly from the optimization cost (1). Instead, we used another mismatched mutual information by assuming that $\tilde{Q}(\hat{X}_n|X_n)$ is distributed according to a circularly symmetric complex Gaussian distribution with some trainable mean and covariance matrix. Accordingly, we define

$$\tilde{I}_{\text{reg}}(X_n; \hat{X}_n) = \mathbb{E}_{X_n, Y_n} \left[\log_2 \left(\frac{\tilde{Q}(\hat{X}_n|X_n)}{\sum_{k=1}^m P(c_k) \tilde{Q}(\hat{X}_n|c_k)} \right) \right]. \quad (5)$$

We use this mismatched mutual information to compare with the one of classification-based equalizer in (3). One should however consider that $\tilde{I}_{\text{reg}}(X_n; \hat{X}_n)$ underestimates the true mutual information $I(X_n; \hat{X}_n)$ [39], [40].

In many telecommunication scenarios, the main source of distortion is AWGN. In these scenarios, a regression-based equalization with MSE loss of (1) can be quite an optimal choice in terms of training and optimal performance. However, such equalizers are penalized if the statistics of distortion deviates from the one of AWGN. That occurs in optical communication as the optical fiber is nonlinear and dispersive. An example is shown in Fig. 1 where the transmission of 16-QAM data is simulated over a particular optical link. The simulation and transmission setup is detailed in Sec. III. We observe here that because of nonlinear effects, the distortion of each constellation has different statistics.

In one hand, a classification-based equalizer can potentially outperform a regression-based equalizer as it can potentially adapt itself to any channel statistics. In particular, $I_{\Theta_{\text{cl}}^*}(X_n; \hat{X}_n)$ can approach the true $I(X; Y)$ provided that the equalizer $f(\cdot; \Theta)$ has large enough “learning complexity” (e.g. number of parameters and flexibility of $f(\cdot; \Theta)$). In the other hand, a classification-based equalizer has some potential drawbacks. To name some: one potential drawback is that the cost function CEL is independent of the spatial proximity of constellation points is involved. In other words, the CEL penalizes the misclassification between two classes with the same “cost” value, which can potentially impact in the learning process. Also, neglecting this information may slow down the training process, especially at its beginning. Another disadvantage of CEL minimization is that according to [31], the CEL surfaces have less local minima than the square error-based losses (SEL), to which the MSE loss belongs. However, the CEL exhibits stronger gradients than the SEL, which causes overfitting in the systems trained with the CEL, resulting in

SEL's having a better generalization property in almost all the cases tested in [31].¹

In the next section, we compare the performance and training complexity of classification and regression in the framework of equalization for optical communication.

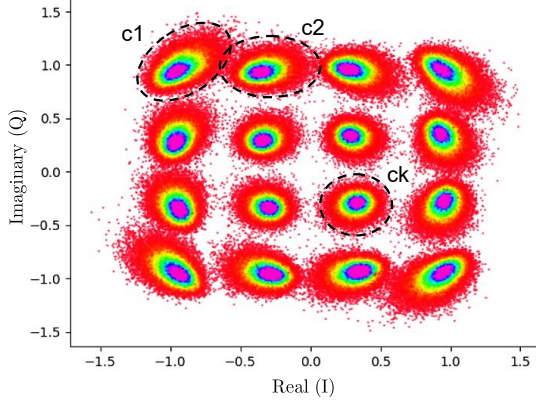


Fig. 1: Distribution of the received symbols in an ideal transmitter of SC-DP 16-QAM case with launch power -1 dBm and 34.4GBd using 9x50km TWC fiber.

B. Equalizers based on Neural Networks

Before moving on to the results section, we discuss how we make the comparison of regression and classification as fair as possible. First, we use two types of equalizers: the first is based on the feed-forward multi-layer perceptron (MLP) with three hidden layers, while the second one is the recurrent structure, consisting of one layer of bidirectional Long short-term memory (biLSTM). The comparison of these equalizers' complexity and functioning is given in Ref. [11]. These two cases are taken to demonstrate that our outcomes are true for different NN architectures, but we note that the biLSTM layer has demonstrated better performance in previous studies [11]. The only difference between using each architecture for regression or classification tasks is the structure of the output layer, as shown in Fig 2, and the loss function type. In the case of regression, the output layer has two linear neurons referring to the real and imaginary parts of the recovered symbol, and the loss function used is the MSE. For the classification, the number of neurons in the output layer is determined by the modulation format cardinality, and the NN structure ends with the softmax layer, while the loss function is the categorical CEL. We point out once more that besides these two differences, the regression and classifier models that we compare, share the same number of inputs, hidden layers, neurons in each layer, and hyperparameter values; the training/test datasets are also the same. As for memory size, for

¹Another drawback of classification-based systems is that it is tailored to each task, i.e. it has to have the specified fixed number of outputs corresponding to the constellation's cardinality. This indicates that the classifier model's operation is specific to the modulation format on which it was trained, the feature which inhibits the practical (say, hardware) classifier implementation. But in the case of regression [41], [42], we do not need to retrain the model at all for it to work on other modulation formats. Because of this, the regression model is far more adaptive than the classification one.

both prediction types, we used the same memory: $M = 51$ for the SSMF case and $M = 41$ for the TWC case. The summary of the NN parameters used in this study is presented in Table. I.

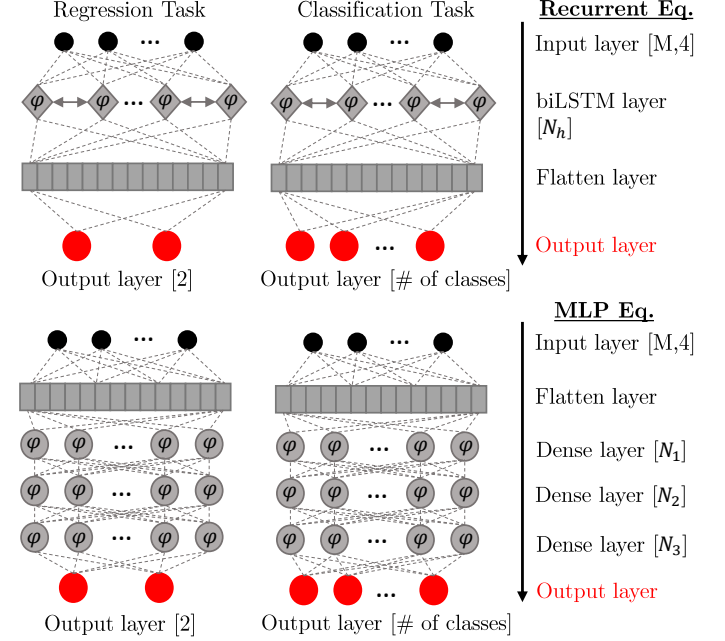


Fig. 2: Schemes of different NN architectures considered in this paper. At the top, we show the regression and classification systems based on the recurrent equalizer with N_h hidden units. At the bottom, we also show both tasks implemented with the MLP equalizer having three hidden layers, with N_1 , N_2 , and N_3 neurons in each consecutive layer, respectively. In all cases, the output is marked with red to highlight the difference in the regression- and classification-based approaches. For our case, the activation function φ is “tanh”.

As we are dealing with different loss functions, we must consider that the learning rate and the number of epochs required may differ for the regression compared to the classification. To address this potential issue, we optimized the learning rate from the range $[10^{-3}, 5 \cdot 10^{-4}, 10^{-4}, 5 \cdot 10^{-5}]$, and used the early stop to get the architecture that performed the best during the training process. In general, the early stop was used if no improvement was seen after 150 epochs out of the total 5000 training epochs.

TABLE I: The common regression and classification tasks NN hyperparameters used in our study.

Equalizer	Mini-Batch	N_h	$N_1 / N_2 / N_3$	Training / Testing Dataset size
Recurrent	4331	226	-	$10^{18} / 10^{18}$
MLP	4331	-	481 / 31 / 263	$10^{18} / 10^{18}$

III. SIMULATING SIGNAL PROPAGATION IN COHERENT OPTICAL TRANSMISSION SYSTEMS

To illustrate the effects addressed in our work, we numerically simulated the dual-polarization (DP) transmission

of a single-channel signal at a 34.4 GBd rate. First, a bit sequence was generated using the Mersenne twister generator [43], which has the periodicity equal to $2^{19937} - 1$. Then, the signal is pre-shaped with a root-raised cosine (RRC) filter with 0.1 roll-off at an upsampling rate of 8 samples per symbol. In addition, the signal could have four possible modulation formats: 16 / 32 / 64-QAM. To cover different physical scenarios, we considered the following two test cases: (i) the transmission over the optical link consisting of 9×50 km true-wave classic (TWC) spans; and (ii) transmission over 5×100 km of standard single-mode fiber (SSMF) spans. The optical signal propagation along the fiber was simulated by solving the Manakov equation via split-step Fourier method [44] with the resolution of 1 km per step². The parameters of the TWC fiber are: the attenuation parameter $\alpha = 0.23$ dB/km, the dispersion coefficient $D = 2.8$ ps/(nm·km), and the effective nonlinearity coefficient $\gamma = 2.5$ (W·km)⁻¹. The SSMF parameters are: $\alpha = 0.2$ dB/km, $D = 17$ ps/(nm·km), and $\gamma = 1.2$ (W·km)⁻¹. The purpose of testing two different fibers is to see if the regression task works better in the SSMF transmission because, due to the dispersion, the constellation points distributions, in that case, would be closer to Gaussian; for the TWC we have 6 times lower dispersion and 2 times higher nonlinearity, such that the non-Gaussianity would be more pronounced.

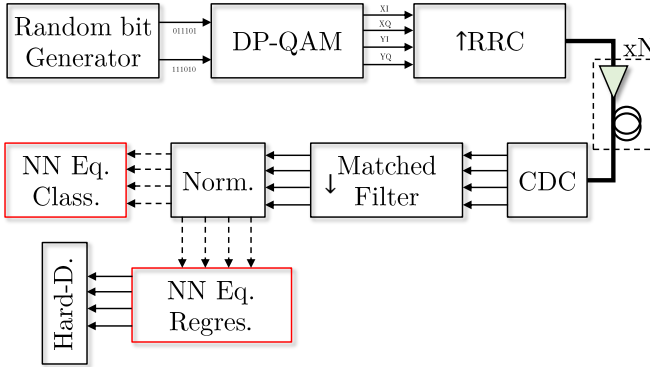


Fig. 3: The schematic of the setup used in our simulations. The two available equalization types (classification and regression) are inserted at the receiver side after the matching filter and the DSP blocks: CDC and Phase/Amplitude Normalization. The equalizers are highlighted with a red box.

In our model, every span is followed by an optical amplifier with the noise figure $NF = 4.5$ dB, which fully compensates for the fiber losses and adds the ASE noise. At the receiver, a standard Rx-DSP was used. It includes the full electronic chromatic dispersion compensation (CDC) using a frequency-domain equalizer, the application of a matched filter, and downsampling to the symbol rate. Finally, the received symbols were normalized (by phase and amplitude) to the transmitted ones. After the Rx-DSP, the output symbols were processed by an NN-based equalizer

for further signal enhancement. Fig. 3 shows all the blocks involved in the transmission simulations, where we highlight regression/classification-based NN equalizers with red boxes. Besides the MI, another performance metric used in this paper is the Q-factor expressed through BER after the hard decision as:

$$Q = 20 \log_{10} \left[\sqrt{2} \operatorname{erfc}^{-1}(2BER) \right], \quad (6)$$

where erfc^{-1} is the inverse complementary error function. Note that the hard-decision block is optional: it is used for the Q-factor computation, but redundant when we deal with the MI.

The NN input mini-batch shape, for both regression and classification tasks, can be defined by three dimensions [11]: $(B, M, 4)$, where B is the mini-batch size, M is the memory size defined through the number of neighbors N as $M = 2N + 1$, and 4 is the number of features for each symbol, referring to the real and imaginary parts of two polarization components. For the regression, the output target is to recover the real and imaginary parts of the k -th symbol in one of the polarization, so the shape of the NN output batch can be expressed as $(B, 2)$. In the case of classification, the output will provide the vector probability of a received symbol to belong to a certain class, and so the output batch shape is equal to (B, MF) . Finally, we note that the different random seeds were used to produce both the training and testing datasets to ensure their independence and avoid overestimation, with the cross-correlation not exceeding 0.02.

IV. COMPARISON OF EQUALIZERS BASED ON REGRESSION OR CLASSIFICATION

A. Performance Comparison

To test the importance of differentiating the output label errors, which takes place in the regression as opposed to the classification, we numerically simulated the transmission of a single-channel (SC) DP 34.4 GBd signal with RRC 0.1 roll-off pulse over a system consisting of 5×100 km SSMF spans at 6 and 10 dBm launch power with different modulation formats: 16-QAM, 32-QAM, and 64-QAM. In this first test, since only the modulation format changes, but we do not have any difference in nonlinearity strength, the goal is to show that when we increase the modulation format, the classifier's performance degrades because the categorical cross-entropy loses the information related to the miss-classification of different label types, and values every misclassification occurrence equally.

The comparison of the regression- and classification-based (*but otherwise equivalent*) systems' performance for different modulation format orders is depicted in Fig. 4. From the results of Fig. 4 (a) and (c), one can see the impact on the classifier's performance when increasing the number of classes in the problem (i.e. increasing the modulation format order), in terms of the Q-factor for 6 and 10 dBm respectively.

For the biLSTM equalizer, the percentage of how greater the Q-factor is after the regression equalization compared to the classification one was roughly 8%, 31%, and 31% for the 16-QAM, 32-QAM, and 64-QAM scenarios, respectively, for

²The fine step resolution guarantees that we truly model the optical channel properties captured by the NN and not address some by-side simulation effects.

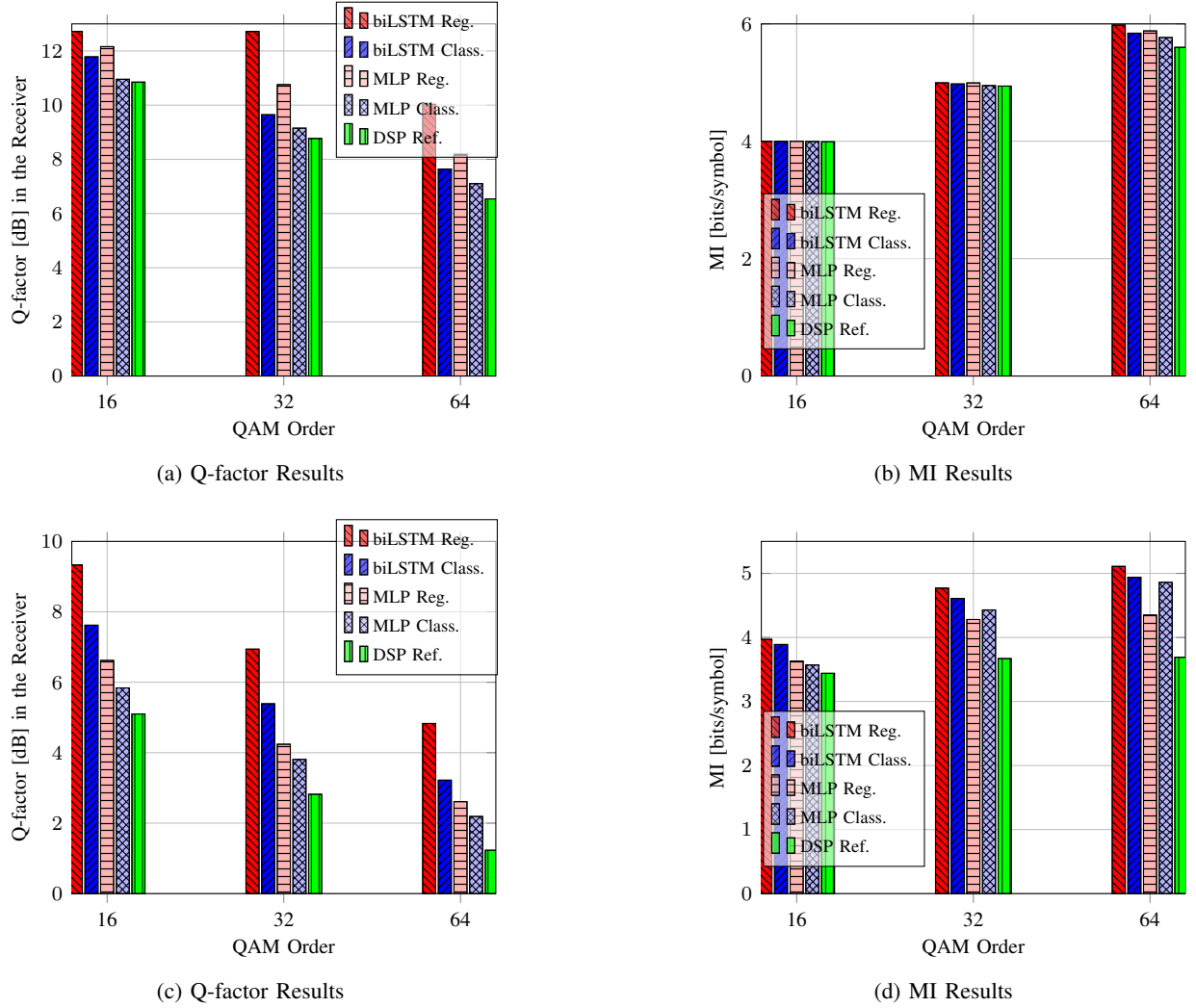


Fig. 4: Performance study for regression and classification equalizer in different modulation format [16-QAM, 32-QAM and 64-QAM] transmission at (a,b) 6 dBm and (c,d) 10dBm SC-DP, 5x100km SSMF fiber and 34.4GBd.

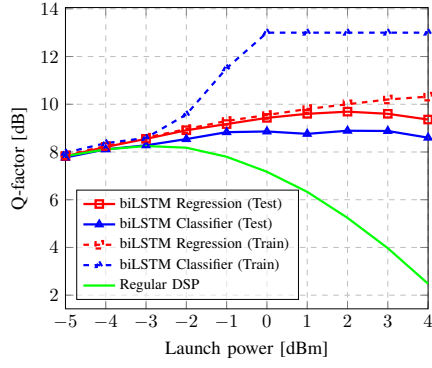
the 6 dBm test case, Fig. 4 (a), and 22%, 29%, and 50% for the 16-QAM, 32-QAM, and 64-QAM scenarios, respectively, for the 10 dBm test case, Fig. 4 (c). For the MLP equalizer, as compared to the classification output in 16-QAM, 32-QAM, and 64-QAM scenarios, the regression equalization always delivered better results, yielding 14%, 19%, and 15% Q-factor improvement, respectively for the 6 dBm test case, Fig. 4 (a), and 7%, 11%, and 19% Q-factor improvement, respectively, for the 10 dBm test case, Fig. 4 (c). When using the biLSTM equalizers, we can observe a greater difference between the regression and classification for different modulation formats, because the biLSTM equalizers, on average, perform much better than the MLP equalizers [11], [45]. So, in the biLSTM case, we can see better how much the classification loss function gets degraded by ignoring the difference between distinct miss-classification occurrences.

When evaluating the performances in terms of MI, almost the same behavior was observed: the results are depicted in Fig. 4 (b) and (d) for 6 and 10 dBm, respectively. In the case of the biLSTM equalizer, the difference between the MI obtained through regression and classifier for 16-, 32-, and 64-QAM

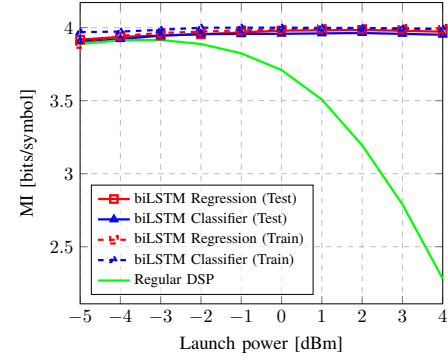
was approximately 0, 0.0191, and 0.1393, for 6 dBm; and 0.0815, 0.161, and 0.1733, for 10 dBm. Again, by increasing the order of the modulation format, the regression achieved better results than the classifiers.

In the case of 6 dBm with the MLP equalizer, the same tendency appeared again: the MI difference was larger when the modulation order increased. The difference between the MI for regression vs. classification was 0.00445, 0.0449, and 0.1126, for modulation formats 16-, 32-, and 64-QAM, respectively. However, when comparing the MLP equalizers' outcomes, the classifier MI was somewhat higher than that for the regression case in two scenarios at 10 dBm: for 32- and 64-QAM cases. We believe that this happened because the MI of the regression is lower-bounded but not computed exactly, and so the MI value estimated via Eq. (5) and Gaussian approximation, is lower than the true one. This is also corroborated by the fact that when we look at the MLP Q-factor for those cases, we still observe the higher Q-factors attributed to the regression model.

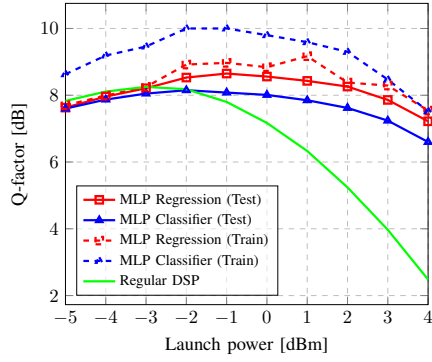
Now we turn to the issue of overfitting in the classification equalizer, addressing two cases: i) the case of a low dispersion



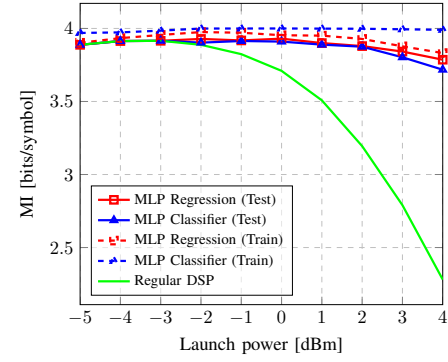
(a) TWC link - biLSTM Equalizer - Q-factor Metric



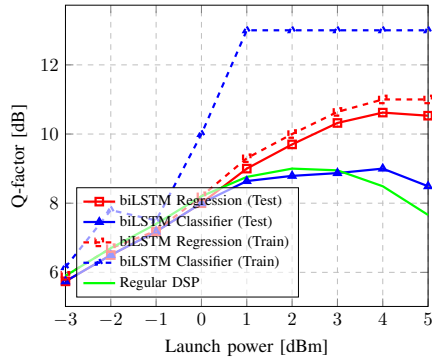
(b) TWC link - biLSTM Equalizer - MI Metric



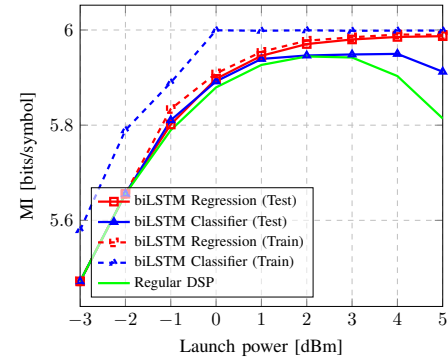
(c) TWC link - MLP Equalizer - Q-factor Metric



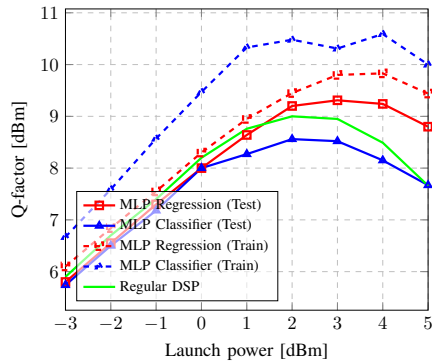
(d) TWC link - MLP Equalizer - MI Metric



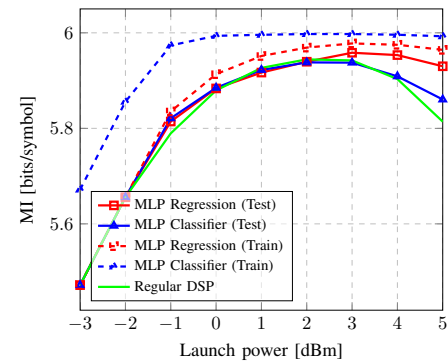
(e) SSMF link - biLSTM Equalizer - Q-factor Metric



(f) SSMF link - biLSTM Equalizer - MI Metric



(g) SSMF link - MLP Equalizer - Q-factor Metric



(h) SSMF link - MLP Equalizer - MI Metric

Fig. 5: Generalization study for regression and classification equalizer showing the impact of overfitting in the NN performance and training process on the following scenarios: (a,b) biLSTM analyses and (c,d) MLP analyses for SC-DP-16-QAM, 9x50km TWC fiber and 34.4GBd; (e,f) biLSTM analyses and (g,h) MLP analyses for SC-DP-64-QAM, 5x100km SSMF fiber and 34.4GBd.

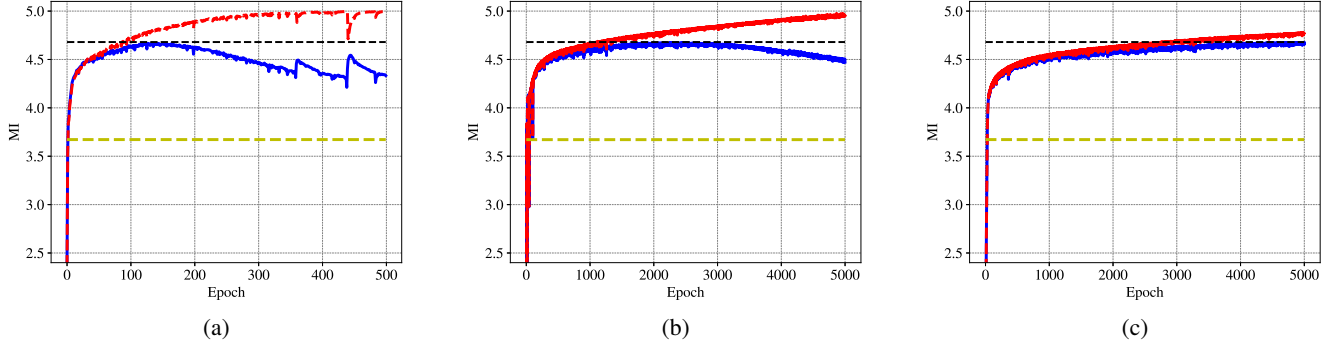


Fig. 6: The performance (MI) versus training epochs for the 32-QAM SSMF 10 dBm case using the biLSTM equalizer with learning rate equal to (a) 10^{-3} , (b) 10^{-4} , and (c) 5×10^{-5} . The red solid curve is the training performance, the blue solid curve is the test performance, the green dashed line is the reference performance when only the linear equalization is implemented, and the black dashed line is the reference for the maximum MI achieved by the testing dataset over the training epochs.

fiber (SC-DP 16QAM 34.4 GBd over 9x50km TWC fiber), and ii) the case of a conventional SSMF fiber (SC-DP 64QAM 34.4 GBd over 5x100km SSMF fiber). To reveal the overfitting, for both the biLSTM and MLP equalizers, we present the Q-factor/MI values for the training and test (validation) datasets. The difference between the values obtained in training and testing is the qualitative measure of the overfitting strength. In these words, the comparison of classification and regression training and testing results will reveal which approach has generalized better. Fig. 5 shows the results of our analysis where the solid green line is the Q-factor/MI after only linear equalization (regular DSP), the solid blue and red lines indicate the Q-factor/MI of the classification and regression models evaluated with the testing dataset, respectively, and the dashed blue and red lines depict the Q-factor/MI of the classification and regression models evaluated with the training dataset.

When we use the CEL in our equalizers, we see the same trend of higher overfitting level as it was observed in Ref. [31]. As can be seen in all four panels, the Q-factor curves of training and testing for the classifiers show a significant difference (since this metric gives the logarithmic measure), suggesting the presence of noticeable overfitting in the classification model.

Then, we can see that, in comparison to the classifier's result, the training and testing output curves when using the regression, behave almost identically. It means that the regression model using MSE generalizes much better for all of our test cases (two different NN equalizers and two different transmission setups), which complies with the conclusions reached in Ref. [31]. Furthermore, we were able to see that by using regression equalizers, the Q-factor level after equalization was still higher than with the classification, due to the better generalization of the regression NNs. When we look at the MI values, we see that the classifier's training performance was overfitted, yielding virtually the maximum MI attainable for each scenario, but in the case of regression, the training and testing curves followed the same trend, indicating a better generalization of the problem.

Finally, we notice that for high modulation formats, such as

those shown in Fig. 1, we have an even more reduced classification performance, with no increase in Q-factor observed for both biLSTM and MLP equalizers in 64-QAM 5x100 SSMF transmission scenario.

B. Training Complexity Comparison

In this final subsection, we highlight the training process of all equalizers used in this paper, considering not only the problem of overfitting but also the speed of convergence for such equalizers.

First, we compare how many epochs each task required to reach the best possible result. For some selected cases discussed in our paper, Table. II displays the training time for the biLSTM and MLP equalizers. When comparing the regression and classification in terms of the number of epochs required to obtain the highest Q-factor, no significant difference in training time was identified, at first. However, for roughly the same amount of training epochs, we can affirm that the regression was more successful because it delivered greater performance outputs.

TABLE II: Summary of the main features in the Regression and Classification tasks.

Test Scenario	Epoch biLSTM Class.	Epoch biLSTM Regress.	Epoch MLP Class.	Epoch MLP Regress.
SSMF 16-QAM 10dBm	385	277	257	153
SSMF 32-QAM 10dBm	147	117	290	512
SSMF 64-QAM 10dBm	462	414	399	391
SSMF 64-QAM 4dBm	279	302	363	95
TWC 16-QAM 2dBm	102	87	152	114

Finally, we would like to note out that when we lowered the learning rate, we saw a reduction in overfitting in the classification task. Fig. 6 shows the example case of 32-QAM at 10 dBm using the SSMF link, where three training and testing MI curves for the biLSTM equalizer are shown for the three learning rates: 10^{-3} , 10^{-4} , and 5×10^{-5} . As can

be seen, for 10^{-3} the overfitting is much more intense than when using lower learning rates. However, even with such low learning rates as 5×10^{-5} , the performance after 5000 epochs of training, was not better than that with either the regression or compared to the best case with the classification with 10^{-3} learning rate. Also, the overfitting could be seen as the training ML level grew faster than the testing level. The maximum MI measured with the test dataset is shown by the black dashed line in Fig. 6. It is evident from this figure that lowering down the learning rate did not result in any considerable improvement for our test cases.

V. CONCLUSION

In this work, we compared the performance and training complexity of the regression and classification predictive models for the use case of post equalization in coherent optical links. We considered several different transmission scenarios including three different modulation formats in two different optical link test-benches with different nonlinear and dispersion responses. The applied equalizers were based on two different architectures: feed forward neural networks and recurrent neural networks. For regression and classification tasks, the equalizers had the same structure, except the last layer. In all these scenarios, the equalizers based on regression outperforms the one based on classification providing higher Q-factor and mutual information. We have further observed that the equalizers based on classification required more careful training as they were more prone to overfitting than the other ones. This observation regarding overfitting is in line with findings from Ref. [31] showing the performance advantage of regression models over classification models in different context, due to the better generalization capability of the former.

We should emphasize that although we have observed a common performance trend between these two predictive models, a general conclusion cannot be made. For instance, some suitable regularization or more problem-specific loss functions may potentially hinder overfitting in the classification case. The scope of this work was to evaluate the performance of the typical classifier and regression architectures with their conventional loss function.

We should further emphasize that both the regression and classification tasks have certain limitations. The regression loss function (the MSE) is a special case of the classification loss function (the CEL), in which the stochastic component of the output variables is assumed to be signal-independent and normally distributed. Therefore, the MSE does not take into account the signal-dependent stochastic contribution, which is, obviously, present in the true nonlinear optical channel. Nonetheless, we underline that from the machine learning methods' application perspective, the classification loss function (the CEL) is unaware of the difference in misclassifying the labels and does not account for the output location in the target space (i.e. of the location of the equalized point on the constellation plane). It seems that the labels-aware misclassification occurrence, pertaining to the regression task, contains important information that impacts the equalization

quality, while this information is lost in the classification-based equalization. Furthermore, according to recent Ref. [31], the CEL landscape typically involves very sharp local minima, which can cause the NN model to overfitting, such that it typically generalizes much worse than the regression model with the loss based on the euclidean distance.

REFERENCES

- [1] E. Agrell, M. Karlsson, A. R. Chraplyvy, D. J. Richardson, P. M. Krummrich, P. Winzer, K. Roberts, J. K. Fischer, S. J. Savory, B. J. Eggleton, M. Secondini, F. R. Kschischang, A. Lord, J. Prat, I. Tomkos, J. E. Bowers, S. Srinivasan, M. Brandt-Pearce, and N. Gisin, "Roadmap of optical communications," *Journal of Optics*, vol. 18, no. 6, p. 063002, may 2016.
- [2] P. J. Winzer, D. T. Neilson, and A. R. Chraplyvy, "Fiber-optic transmission and networking: the previous 20 and the next 20 years," *Optics Express*, vol. 26, no. 18, pp. 24 190–24 239, 2018.
- [3] J. C. Cartledge, F. P. Guiomar, F. R. Kschischang, G. Liga, and M. P. Yankov, "Digital signal processing for fiber nonlinearities," *Optics Express*, vol. 25, no. 3, pp. 1916–1936, Feb 2017.
- [4] T. O'Shea and J. Hoydis, "An introduction to deep learning for the physical layer," *IEEE Transactions on Cognitive Communications and Networking*, vol. 3, no. 4, pp. 563–575, 2017.
- [5] S. Dörner, S. Cammerer, J. Hoydis, and S. Ten Brink, "Deep learning based communication over the air," *IEEE Journal of Selected Topics in Signal Processing*, vol. 12, no. 1, pp. 132–143, 2017.
- [6] S. Deligiannidis, A. Bogris, C. Mesaritakis, and Y. Kopsinis, "Compensation of fiber nonlinearities in digital coherent systems leveraging long short-term memory neural networks," *Journal of Lightwave Technology*, vol. 38, no. 21, pp. 5991–5999, 2020.
- [7] M. Schaedler, F. Pittala, G. Böcherer, C. Bluemm, M. Kuschnerov, and S. Pachnicke, "Recurrent neural network soft-demapping for nonlinear isi in 800gbit/s dwdm coherent optical transmissions," in *46th European Conference on Optical Communication (ECOC 2020)*, 2020.
- [8] F. N. Khan, C. Lu, and A. P. T. Lau, "Machine learning methods for optical communication systems," *Optical Society of America*, 2017, p. SpW2F3.
- [9] D. Zibar, M. Piels, R. Jones, and C. G. Schäeffler, "Machine learning techniques in optical communication," *Journal of Lightwave Technology*, vol. 34, no. 6, pp. 1442–1452, 2016.
- [10] F. Musumeci, C. Rottondi, A. Nag, I. Macaluso, D. Zibar, M. Ruffini, and M. Tornatore, "An overview on application of machine learning techniques in optical networks," *IEEE Communications Surveys Tutorials*, vol. 21, no. 2, pp. 1383–1408, 2019.
- [11] P. J. Freire, Y. Osadchuk, B. Spinnler, A. Napoli, W. Schairer, N. Costa, J. Prilepsky, and S. K. Turitsyn, "Performance versus complexity study of neural network equalizers in coherent optical systems," *Journal of Lightwave Technology*, pp. 1–1, 2021.
- [12] M. A. Jarajreh, E. Giacomidis, I. Aldaya, S. T. Le, A. Tsokanos, Z. Ghassemlooy, and N. J. Doran, "Artificial neural network nonlinear equalizer for coherent optical ofdm," *IEEE Photonics Technology Letters*, vol. 27, no. 4, pp. 387–390, 2015.
- [13] D. Wang, M. Zhang, Z. Li, C. Song, M. Fu, J. Li, and X. Chen, "System impairment compensation in coherent optical communications by using a bio-inspired detector based on artificial neural network and genetic algorithm," *Optics Communications*, vol. 399, pp. 1–12, 2017.
- [14] C. Häger and H. D. Pfister, "Nonlinear interference mitigation via deep neural networks," in *2018 Optical Fiber Communications Conference and Exposition (OFC)*. IEEE, 2018, pp. 1–3.
- [15] C. Huang, S. Fujisawa, T. F. de Lima, A. N. Tait, E. Blow, Y. Tian, S. Bilodeau, A. Jha, F. Yaman, H. G. Batshon, H. Peng, B. J. Shastri, Y. Inada, T. Wang, and P. R. Prucnal, "Demonstration of photonic neural network for fiber nonlinearity compensation in long-haul transmission systems," in *2020 Optical Fiber Communications Conference and Exhibition (OFC)*, 2020, pp. 1–3.
- [16] B. I. Bitachon, A. Ghazisaeidi, M. Eppenberger, B. Baeuerle, M. Ayata, and J. Leuthold, "Deep learning based digital backpropagation demonstrating snr gain at low complexity in a 1200km transmission link," *Optics Express*, vol. 28, no. 20, pp. 29 318–29 334, Sep 2020.
- [17] Y. Zhao, X. Chen, T. Yang, L. Wang, D. Wang, Z. Zhang, and S. Shi, "Low-complexity fiber nonlinearity impairments compensation enabled by simple recurrent neural network with time memory," *IEEE Access*, vol. 8, pp. 160 995–161 004, 2020.

- [18] M. M. Melek and D. Yevick, "Nonlinearity mitigation with a perturbation based neural network receiver," *Optical and Quantum Electronics*, vol. 52, no. 10, pp. 1–10, 2020.
- [19] S. Zhang, F. Yaman, K. Nakamura, T. Inoue, V. Kamalov, L. Jovanovski, V. Vusirikala, E. Mateo, Y. Inada, and T. Wang, "Field and lab experimental demonstration of nonlinear impairment compensation using neural networks," *Nature communications*, vol. 10, no. 1, pp. 1–8, 2019.
- [20] P. J. Freire, V. Neskornuik, A. Napoli, B. Spinnler, N. Costa, G. Khanna, E. Riccardi, J. E. Prilepsky, and S. K. Turitsyn, "Complex-valued neural network design for mitigation of signal distortions in optical links," *Journal of Lightwave Technology*, vol. 39, no. 6, pp. 1696–1705, 2021.
- [21] B. Karanov, P. Bayvel, and L. Schmalen, "End-to-end learning in optical fiber communications: Concept and transceiver design," in *2020 European Conference on Optical Communications (ECOC)*, 2020, pp. 1–4.
- [22] B. Karanov, M. Chagnon, F. Thouin, T. A. Eriksson, H. Bülow, D. Lavery, P. Bayvel, and L. Schmalen, "End-to-end deep learning of optical fiber communications," *Journal of Lightwave Technology*, vol. 36, no. 20, pp. 4843–4855, 2018.
- [23] Z.-R. Zhu, J. Zhang, R.-H. Chen, and H.-Y. Yu, "Autoencoder-based transceiver design for owc systems in log-normal fading channel," *IEEE Photonics Journal*, vol. 11, no. 5, pp. 1–12, 2019.
- [24] K. Gümüş, A. Alvarado, B. Chen, C. Häger, and E. Agrell, "End-to-end learning of geometrical shaping maximizing generalized mutual information," in *2020 Optical Fiber Communications Conference and Exhibition (OFC)*, 2020, pp. 1–3.
- [25] F. A. Aoudia and J. Hoydis, "End-to-end learning for ofdm: From neural receivers to pilotless communication," *arXiv preprint arXiv:2009.05261*, 2020.
- [26] V. Neskornuik, A. Carnio, V. Bajaj, D. Marsella, S. K. Turitsyn, J. E. Prilepsky, and V. Aref, "End-to-end deep learning of long-haul coherent optical fiber communications via regular perturbation model," in *ECOC 2021*, 2021.
- [27] S. Dreiseitl and L. Ohno-Machado, "Logistic regression and artificial neural network classification models: a methodology review," *Journal of Biomedical Informatics*, vol. 35, no. 5, pp. 352–359, 2002.
- [28] J. Vallejos and S. McKinnon, "Logistic regression and neural network classification of seismic records," *International Journal of Rock Mechanics and Mining Sciences*, vol. 62, pp. 86–95, 2013.
- [29] P. Golik, P. Doetsch, and H. Ney, "Cross-entropy vs. squared error training: a theoretical and experimental comparison," in *Interspeech*, vol. 13, 2013, pp. 1756–1760.
- [30] K. Nar, O. Ocal, S. S. Sastry, and K. Ramchandran, "Cross-entropy loss leads to poor margins," 2018.
- [31] A. S. Bosman, A. Engelbrecht, and M. Helbig, "Visualising basins of attraction for the cross-entropy and the squared error neural network loss functions," *Neurocomputing*, vol. 400, pp. 113–136, 2020.
- [32] S. Lathuilière, P. Mesejo, X. Alameda-Pineda, and R. Horaud, "A comprehensive analysis of deep regression," *IEEE transactions on pattern analysis and machine intelligence*, vol. 42, no. 9, pp. 2065–2081, 2019.
- [33] Y. Li, C. Lan, J. Xing, W. Zeng, C. Yuan, and J. Liu, "Online human action detection using joint classification-regression recurrent neural networks," in *European conference on computer vision*. Springer, 2016, pp. 203–220.
- [34] L. Mukherjee, M. A. K. Sagar, J. N. Ouellette, J. J. Watters, and K. W. Eliceiri, "Joint regression-classification deep learning framework for analyzing fluorescence lifetime images using nadh and fad," *Biomedical Optics Express*, vol. 12, no. 5, pp. 2703–2719, 2021.
- [35] M. Liu, J. Zhang, E. Adeli, and D. Shen, "Joint classification and regression via deep multi-task multi-channel learning for alzheimer's disease diagnosis," *IEEE Transactions on Biomedical Engineering*, vol. 66, no. 5, pp. 1195–1206, 2018.
- [36] —, "Deep multi-task multi-channel learning for joint classification and regression of brain status," *International conference on medical image computing and computer-assisted intervention*, pp. 3–11, 2017.
- [37] J.-Y. Wu, M. Wu, Z. Chen, X. Li, and R. Yan, "A joint classification-regression method for multi-stage remaining useful life prediction," *Journal of Manufacturing Systems*, vol. 58, pp. 109–119, 2021.
- [38] J. Chen, L. Cheng, X. Yang, J. Liang, B. Quan, and S. Li, "Joint learning with both classification and regression models for age prediction," in *Journal of Physics: Conference Series*, vol. 1168, no. 3. IOP Publishing, 2019, p. 032016.
- [39] N. Merhav, G. Kaplan, A. Lapidoth, and S. S. Shitz, "On information rates for mismatched decoders," *IEEE Transactions on Information Theory*, vol. 40, no. 6, pp. 1953–1967, 1994.
- [40] P. J. Freire, D. A. Abode, J. E. Prilepsky, N. Costa, B. Spinnler, A. Napoli, and S. K. Turitsyn, "Transfer learning for neural networks-based equalizers in coherent optical systems," *Journal of Lightwave Technology*, pp. 1–1, 2021.
- [41] P. J. Freire, D. A. Abode, J. E. Prilepsky, and S. K. Turitsyn, "Power and modulation format transfer learning for neural network equalizers in coherent optical transmission systems," in *OSA Advanced Photonics Congress 2021*, 2021.
- [42] M. Matsumoto and T. Nishimura, "Mersenne twister: a 623-dimensionally equidistributed uniform pseudo-random number generator," *ACM Transactions on Modeling and Computer Simulation (TOMACS)*, vol. 8, no. 1, pp. 3–30, 1998.
- [43] G. P. Agrawal, *Nonlinear Fiber Optics*, 5th ed. Boston: Academic Press, 2013.
- [44] P. J. Freire, Y. Osadchuk, B. Spinnler, W. Schairer, A. Napoli, N. Costa, J. E. Prilepsky, and S. K. Turitsyn, "Experimental study of deep neural network equalizers performance in optical links," in *2021 Optical Fiber Communications Conference and Exhibition (OFC)*, 2021, pp. 1–3.